

## Modeling of ZGDC polarization splitter on SiN

© I.V. Kuznetsov, A.S. Perin

Tomsk State University of Control Systems and Radioelectronics, Tomsk, Russia

e-mail: anton.s.perin@tusur.ru

Received May 10, 2023

Revised October 06, 2023

Accepted October 30, 2023

In this work we present results of numerical modeling of a ZGDC polarisation splitter based on SiN thin films. The magnitude of the interference is  $-15$  dB for the TM-mode and  $-10.4$  dB for TE-mode. The transmission coefficient is 43%.

**Keywords:** silicon nitride, polarisation splitter, directional coupler, two-mode interference, photonic integrated circuit.

DOI: 10.61011/EOS.2023.11.58040.5003-23

Polarization splitter (PS) — is a passive optical device that performs spatial separation of TE and TM modes. The PS can be used as an element in communication systems that use channel separation by polarization or as an element of a photonic integrated circuit (PIC), ensuring the joining of polarization-dependent PIC elements [1–3].

The most widespread are integrated PS based on the silicon-on-insulator (SOI) platform [1–3]. The SOI platform provides low scattering losses into the cladding due to high refraction index contrast. One of the advantages of SOI is also its compatibility with CMOS technologies. The disadvantage of the SOI platform is the opacity of silicon in the visible part of the optical spectrum, which does not allow the use of SOI-based PIC visible light communication devices [4–6]. In addition, silicon may experience nonlinear optical losses caused by two-photon absorption in the near-infrared spectrum [6–8].

Thus, an urgent task is to study the use of alternative materials for the development and production of passive PIC elements. One of the promising materials is silicon nitride ( $\text{Si}_3\text{N}_4$ ). Like silicon,  $\text{Si}_3\text{N}_4$  is a CMOS-compatible material, but is not subject to two-photon absorption, has a wider range of optical transparency, and lower wall roughness [6]. Currently,  $\text{Si}_3\text{N}_4$  is used to create various passive PIC elements, for example, ring resonators, mode converters, coupling elements, optical filters, etc. [9].

The aim of this work is the numerical modeling of a PS based on comb waveguides made of thin films  $\text{Si}_3\text{N}_4$ . The main task is to determine the configuration corresponding to the highest division efficiency, the shortest length and the least crosstalk.

Methods for implementing integrated polarization dividers based on directional couplers are known from the literature [10,11]. A directional coupler consists of two waveguides having a coupling section of length  $L$  and characterized by the distance between the waveguides along the coupling section ( $w_g$ ). The layout of such a splitter is shown in Fig. 1, *a*.

In this work, we consider a PS based on a zero gap directional coupler, characterized in that instead of two closely spaced parallel waveguides, between which mode flow is observed, one waveguide is formed, the width of which is 2 times greater than the width of the input and output waveguides ( $w$ ). The layout of such a polarization divider is shown in Fig. 1, *b*.

One of the main advantages of a PS based on a zero gap directional coupler is the absence of additional internal walls of the waveguides in the area of their coupling. It is known [12,13] that the roughness of the interfaces between media is responsible for most of the optical losses in comb waveguides made by plasma-chemical etching [14]. The effect of polarization separation in such a waveguide is achieved due to the interference of symmetric (fundamental) and asymmetric (first-order) modes [11]. Since TE and TM modes have different effective refraction indices (ERI), they form different interference patterns; accordingly, the length of the two mode interference zone  $L$  determines the flow of radiation into one of the output waveguides.

The polarization splitter model under review is based on comb waveguides formed from thin films of  $\text{Si}_3\text{N}_4$  on a silicon dioxide insulator ( $\text{SiO}_2$ ). The parameters of numerical simulation are shown in Table 1.

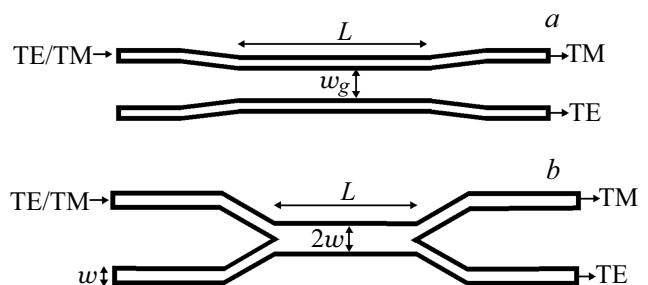


**Figure 1.** Typical PS configurations are: *a* — PS based on a conventional directional coupler, *b* — PS based on zero gap directional coupler.

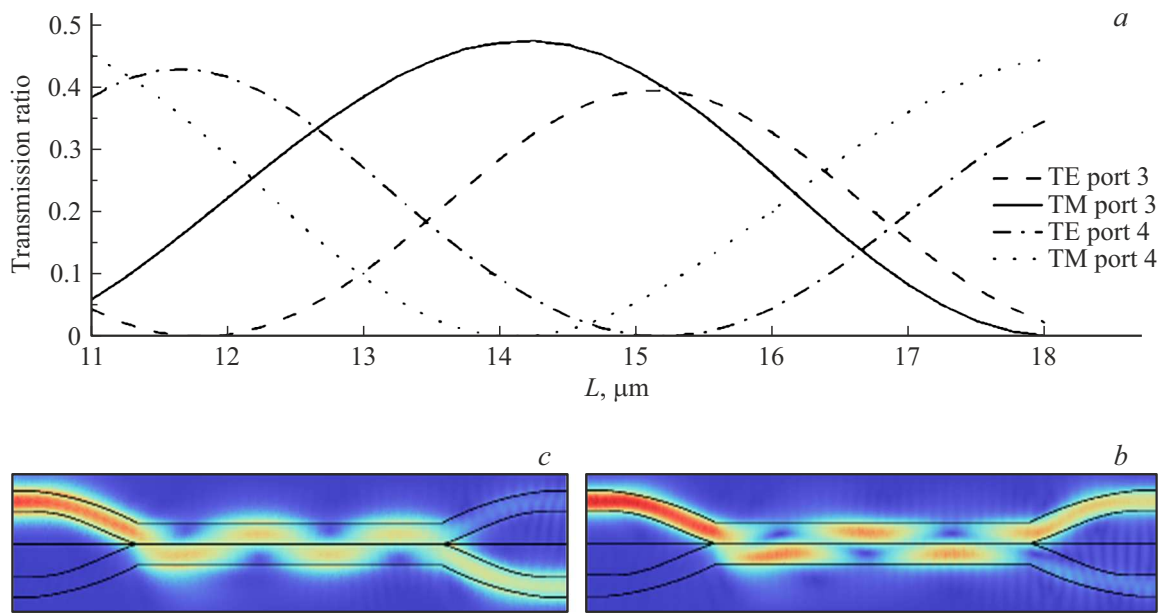


**Figure 2.** Results of numerical simulation: *a* — dependence of the port transmittance coefficient on the type of mode and the length of the two-mode interference zone, *b* — calculation of the propagation of the TE mode for the length of the two-mode interference zone  $14.5 \mu\text{m}$ , *c* — calculation of the propagation of the TM mode with a two-mode interference zone length of  $14.5 \mu\text{m}$ .

The choice of parameters given in Table 1 is determined by existing technological limitations and corresponds to modern data on the manufacture of comb waveguides based on  $\text{Si}_3\text{N}_4$  [17,18].

To calculate the coupling lengths of the TE and TM modes, let us turn to the formula [10,11]

$$L_C^{\text{TE}} = \frac{\lambda}{2\Delta N^{\text{TE}}}, \quad L_C^{\text{TM}} = \frac{\lambda}{2\Delta N^{\text{TM}}},$$

where  $\lambda$  — wavelength,  $\Delta N^{\text{TE}}$ ,  $\Delta N^{\text{TM}}$  — the difference between the ERI of the fundamental TE/TM mode and the ERI of the first order TE/TM mode, respectively. The ERI of the modes were calculated using the finite difference method [19]. Results of the calculation of the coupling length are presented in Table 2.

**Table 1.** Simulation parameters

Parameter	Parameter value
Waveguide width is $w$ , nm	600
Waveguide height, nm	800
Refraction index $\text{Si}_3\text{N}_4$	2 [15]
$\text{SiO}_2$	index 1.44 [16]
Wavelength, $\mu\text{m}$	1.55

**Table 2.** Results of coupling length calculations

$n_{\text{ef}}^{\text{TE0}}$	$n_{\text{ef}}^{\text{TM0}}$	$n_{\text{ef}}^{\text{TE1}}$	$n_{\text{ef}}^{\text{TM1}}$	$\Delta N^{\text{TE}}$	$\Delta N^{\text{TM}}$	$L_C^{\text{TE}}$	$L_C^{\text{TM}}$
1.7823	1.8053	1.5746	1.5843	0.208	0.221	$3.731 \mu\text{m}$	$3.507 \mu\text{m}$

The actual length of the two-mode interference zone can be found using the formula [5]

$$L = mL_c^{\text{TE/TM}},$$

where  $m = 1, 2, 3, \dots$ ,  $L_c^{\text{TE/TM}}$  — is the coupling length of the corresponding mode.

The simulation used a boundary condition that prevented radiation from being reflected back from the outer boundaries of the model. Figure 2, *a* shows the dependence of the transmission coefficient of the output ports on the mode and length of the two-mode interference zone, obtained as a result of numerical simulation. Figure 2, *b* presents the calculation of light propagation through the PS.

Fig. 2, *a–c* shows that with the length of the two-mode interference zone  $L = 14.5 \mu\text{m}$ , separation of TE/TM modes is achieved across different ports. Fig. 3 distribution at the output end of the PS for TE and TM modes at  $L = 14.5 \mu\text{m}$ .

The calculated crosstalk for the TM mode is  $-15 \text{ dB}$ , for the TE mode  $-10.4 \text{ dB}$ , the transmittance coefficient was 43%. The crosstalk obtained is superior to that achieved by a similar configuration based on lithium niobate [11]. The developed PS model can be used in the future for the development of PIC based on  $\text{Si}_3\text{N}_4$  or the hybrid platform  $\text{Si}_3\text{N}_4/\text{Si}$  [6].

Thus, the opportunity of implementing a PS based on comb waveguides made of  $\text{Si}_3\text{N}_4$  thin films in the configuration of a zero gap directional coupler with a two-mode interference length of  $14.5 \mu\text{m}$  was demonstrated. The resulting crosstalk was  $-15 \text{ dB}$  for the TM mode and  $-10.4 \text{ dB}$  for the TE mode.

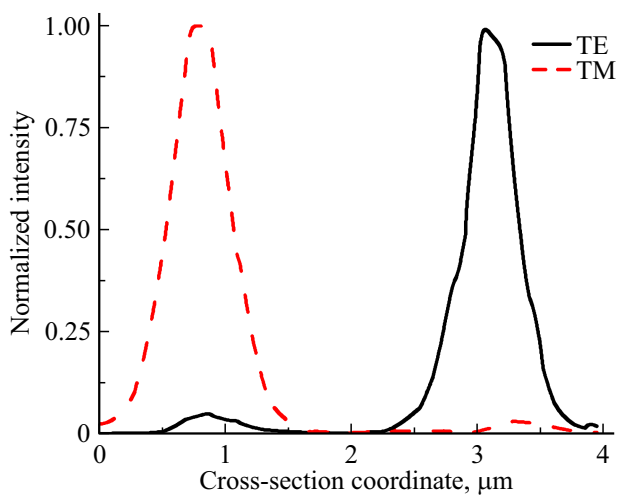


**Figure 3.** Normalized intensity distribution at the output of the PS for TE and TM modes.

### Funding

The research was carried out within the state assignment of Ministry of Science and Higher Education of the Russian Federation (theme No. FEWM-2022-0004).

### Conflict of interest

The authors declare that they have no conflict of interest.

### References

- [1] C.W. Hsu, T.K. Chang, J.Y. Chen, Y.C. Cheng. *Appl. Optics*, **55** (12), 3313 (2016). DOI: 10.1364/AO.55.003313
- [2] L. Liu, Y. Ding, K. Yvind, J.M. Hvam. *Optics Express*, **19** (13), 12646 (2011). DOI: 10.1364/OE.19.012646
- [3] D. Dai, J.E. Bowers. *Optics Express*, **19** (19), 18614 (2011). DOI: 10.1364/OE.19.018614
- [4] L. Matheus, A. Viera, L.F.M. Viera, M.A.M. Viera, O. Gnawali. *IEEE Commun. Surveys & Tutorials*, **21** (4), 3204 (2019). DOI: 10.1109/COMST.2019.2913348
- [5] H. Fukuzawa, J. Yoshinari, H. Hara, K. Sasaki, H. Take, M. Yoshida, T. Kikukawa. *AIP Advances*, **12** (6), 065029 (2022). DOI: 10.1063/5.0088842
- [6] T. Sharma, J. Wang, B.K. Kaushik, Z. Cheng, R. Kumar, Z. Wei, X. Li. *IEEE Access*, **8**, 195436 (2020). DOI: 10.1109/ACCESS.2020.3032186
- [7] A.Z. Subramanian, P. Neutens, A. Dhakal, R. Jansen, T. Claes, X. Rottenberg, F. Peyskens, S. Selvaraja, P. Helin, B. DuBois, K. Leyssens, S. Severi, P. Deshpande, R. Baets, P. Van Dorpe. *IEEE Photonics J.*, **5** (6), 2202809 (2013). DOI: 10.1109/JPHOT.2013.2292698
- [8] H. Ying, S. Junfeng, L. Xianshu, L. Tsung-Yang, L. Guo-Qiang. *Opt. Express*, **22** (18) 21859 (2014).
- [9] D.J. Blumenthal, R. Heideman, D. Geuzebroek, A. Leinse, C. Roeloffzen. *Proc. IEEE*, **106** (12), 2209 (2018). DOI: 10.1109/JPROC.2018.2861576
- [10] M. Kuznetsov. *Optics Lett.*, **8** (9), 499 (1983). DOI: 10.1364/OL.8.000499
- [11] R. Sattibabu, P.K. Dey, B.N. Bhaktha, P. Ganguly. *Results in Optics*, **8**, 100262 (2022). DOI: 10.1016/j.rio.2022.100262
- [12] F.P. Payne, J.P.R. Lacey. *Optical and Quantum Electronics*, **26**, 977 (1994). DOI: 10.1007/BF00708339
- [13] E. Jaberansary, T.M.B. Masaud, M.M. Milosevic, M. Nedeljkovic, G.Z. Mashanovich, H.M.H. Chong. *IEEE Photonics J.*, **5** (3) 6601010 (2013). DOI: 10.1109/JPHOT.2013.2251869
- [14] B.E.E. Kastenmeier, P.J. Matsuo, G.S. Oehrlein. *J. Vacuum Science & Technology A: Vacuum, Surfaces, and Films*, **17** (6), 3179 (1999). DOI: 10.1116/1.582097
- [15] H.R. Philipp. *J. Electrochemical Society*, **120** (2), 295 (1973). DOI: 10.1149/1.2403440
- [16] I.H. Malitson. *JOSA*, **55** (10), 1205 (1965). DOI: 10.1364/JOSA.55.001205
- [17] J.C. Mak, W.D. Sacher, H. Ying, X. Luo, P.G.Q. Lo, J.K. Poon. *Optics Express*, **26** (23), 30623 (2018). DOI: 10.1364/OE.26.030623
- [18] Y. Chen, T.D. Bucio, A.Z. Khokhar, M. Banakar, K. Grabska, F.Y. Gardes, R. Halir, I. Molina-Fernández, P. Cheben, J.J. He. *Optics Lett.*, **42** (18), 3566 (2017). DOI: 10.1364/OL.42.003566
- [19] A.B. Fallahkhair, K.S. Li, T.E. Murphy. *J. Lightwave Technology*, **26** (11), 1423 (2008).

*Translated by E.Potapova*